

Preparation and characterization of the thermoelectric material Zn_4Sb_3

M. VAIDA^{a,*}, N. DUTEANU^a, I. GROZESCU^{a,b}

^aPolitehnica University of Timisoara, Industrial Chemistry and Environmental Engineering Faculty, 6 V. Pirvan Blvd., 300223 Timisoara, Romania

^bNational Institute for Research and Development in Electrochemistry and Condensed Matter, 1 Plautius Andronescu Street, 300224 Timisoara, Romania

The thermoelectric materials gained a lot of attention in the last decades, due to their possible applications. The thermoelectric materials can generate electricity from heat and these materials have an efficiency which depends on the dimensionless figure of merit. Zn_4Sb_3 was reported as an excellent thermoelectric material in an intermediate temperature range (473–673 K). In addition to a promising thermoelectric performance, Zn_4Sb_3 has attracted attention for its other features, such as being an environmentally friendly material and with low costs of production. The aims of this paper are to present the results regarding the obtaining and the characterization of the thermoelectric Zn_4Sb_3 material synthesized by melting a precursors mixture at 1173K for 24 hours, using precursors with a high purity. The obtained material was analyzed and characterized through X-ray diffraction and by specific microscopic techniques as: energy-dispersive X-ray spectroscopy, scanning electron microscopy and atomic force microscopy. The X-ray diffraction pattern show that β - Zn_4Sb_3 was formed. The measured particles dimension on the scanned surfaces is between 2.1 and 3.2 μm . Also, the average roughness - S_a and the root mean squared roughness - S_q were determined.

(Received April 9, 2015; accepted June 24, 2015)

Keywords: Zinc, Antimony, Thermoelectric materials, Melting, Physical properties

1. Introduction

In the last decades, a lot of attention was gained by research studies with the main goal to find alternative energy resources among the existing ones. One of these directions is to obtain materials which can generate electricity from heat, materials known as thermoelectric materials (TE). The efficiency of the heat conversion of the thermoelectric materials is ensured by a low thermal and a high electrical conductivity of these.

Zn_4Sb_3 was reported as an excellent thermoelectric material in an intermediate temperature range (450–670 K) [1]. Beside the promising performance as a thermoelectric material which could make it commercially viable, Zn_4Sb_3 also possess other attractive features as being environmentally friendly and with low costs of production comparative with other materials with the same properties.

According to the existing studies, Zn_4Sb_3 exists in four crystallographic phases: the α -phase which is stable below 263K, the β -phase from 263 K to 765 K, the γ -phase from 765 K to 805 K [2-4] and the γ' from 805K to 839K [3]. It was reported that only the single β -phase has high thermoelectric properties with a value for the figure of merit (ZT), the main measure of the energy conversion performance of the thermoelectric materials, $ZT=1.3$ at 670K [1]).

The figure of merit, Z is defined as:

$$ZT = \alpha^2 \sigma T / \lambda \quad (1)$$

where α is the Seebeck coefficient, T the absolute temperature, σ the electrical conductivity and λ the thermal conductivity [1].

This high efficiency of Zn_4Sb_3 is coming from the remarkably glass-like thermal conductivity. The low thermal conductivity of Zn_4Sb_3 is coming from the high levels of interstitials and from domains of interstitial ordering, leading to disorder at multiple length scales [5].

A lot of researches regarding methods of obtaining Zn_4Sb_3 with a larger figure of merit were tried. In time, were reported different methods in obtaining Zn_4Sb_3 as: melt and quenching [1, 6-12], solid state reaction [13-14], thin films prepared by co-sputtering [15], zone-melting technique [2, 16], melt-spinning technique [17], melting combined with high-energy ball milling [18-19], melting combined with mechanical grinding [20-22], gradient freeze method [23], low temperature solution route [24], etc.

It was also studied the thermal stability of Zn_4Sb_3 [2, 16, 25-27] because this can affect the practical applications if pure samples cannot be obtained. The thermal stability of Zn_4Sb_3 is poor, ZnSb and Zn is formed after the decomposition of the compound which often appear below the expected range of temperature [2, 26-27]. The thermoelectric Zn_4Sb_3 fabricated by zone-melting technique was appreciated by the researchers to be more thermal stable than simple melting and quenching method because it presents a *limited* degradation, which is considered a huge improvement in the thermal stability [2].

Beside the thermal stability, mechanical stability represents another important feature which can influence the thermoelectric properties of the material. It was observed that the bulk material of Zn_4Sb_3 prepared by the traditional melting and quenching in water method suffers microcracks and has very poor mechanical strengths. The mechanical instability occurs due to the volumetric change at the temperature of the phase transition between γ and β phases (765K), the cause being the different thermal expansion coefficients of the γ and β phases [10-11]. Qi *et al.* [17] succeeded in improving the material strength by reducing the average grain size of the material.

Thus, the challenge of improving the thermal stability by choosing an appropriate method to synthesize Zn_4Sb_3 and to increase the mechanical stability of this, remain.

The aims of this paper are to present the results regarding the successfully obtaining of the thermoelectric β - Zn_4Sb_3 material synthesized by melting at 1173K for 24 h to achieve the best thermoelectric performance. The obtained material was analyzed and characterized through X-ray diffraction to establish the structure of this and the morphology and the topography were determined by specific microscopic techniques as scanning electron microscopy / energy-dispersive X-ray spectroscopy and by atomic force microscopy.

2. Experimental details

2.1. Sample preparation

High purity metallic Zn (99.999%, Carlo Erba) and Sb (99%, Carlo Erba) powders were weighed in a stoichiometric ratio of 4:3 with an excess of zinc of 2%. The weighed elements were loaded into a quartz ampoule from which was evacuated the air until a pressure of 10^{-2} bar was obtained. After that, the ampoule was sealed to prevent oxidation during the high temperature in the melting process. The sealed ampoule was placed horizontally into a furnace and heated slowly with a heating rate of the furnace of 323K/h and kept isothermally at 1173 K for 24 hours. The melted alloy was gradually cooled until 873K and then quenched in cold water to form Zn_4Sb_3 compound. To obtain a fine powder, the formed ingots were grounded in an agate mortar.

2.2. Apparatus

To achieve the structural information for Zn_4Sb_3 was used the X-ray diffraction (XRD) (X'pert Pro MPD X-ray diffractometer) using monochromatic Cu $K\alpha$ ($\lambda = 1.5406$ Å) incident radiation over 2θ range of 10 - 65° in

combination with the database of the Joint Committee on Powder Diffraction Standards (JCPDS).

To establish the morphology and the dimension of the particles of the material were used the Scanning Electron Microscopy / Energy-dispersive X-ray spectroscopy (SEM / EDX) (Quanta 250 FEG, mode SE at 30kV accelerating voltage / SDD Apollo X detector) and the Atomic Force Microscopy (AFM) (Model Nanosurf® EasyScan 2 Advanced Research).

3. Results and discussions

The achieved XRD pattern, for the powder obtained from the melting and quenching of the Zn and Sb in stoichiometric ratio, was indexed and compared with the JCPDS database Nos. 00-034-1013. It can be seen that Zn and Sb had been uniformly alloyed and the β - Zn_4Sb_3 phase was obtained, which is in accordance with the previous results [1].

The obtained structure belongs to the rhombohedral space group R-3c, space group nb. 167, where the atomic positions are: 36Zn, 18Sb (1) and 12Sb (2) [4, 28-29].

Fig. 1 presents the XRD pattern of the obtained Zn_4Sb_3 . The very sharp peaks of the XRD pattern indicate a high crystallinity of Zn_4Sb_3 .

A SEM analysis was made to investigate the form and the geometry of the particles. As it can be seen from the SEM images (Fig. 2(a) and Fig. 2 (b)), the particles are agglomerated and asymmetric, oriented in different directions.

In Fig. 2(c) and Fig. 2(d), it can also be observed that the material presents beside dense areas of material, also a certain grade of porosity, porosity reported also in [30] and explained as a result of the explosion of the gases during the synthesis.

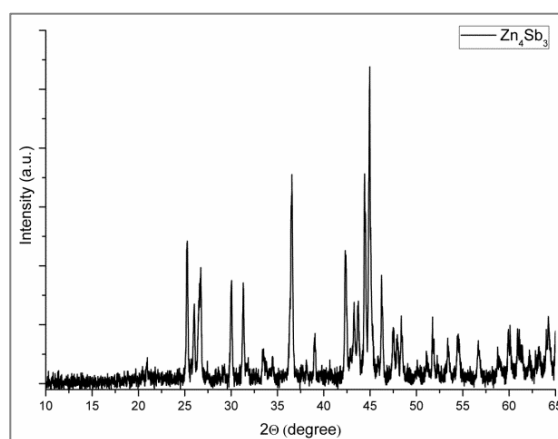


Fig. 1. XRD pattern of β - Zn_4Sb_3

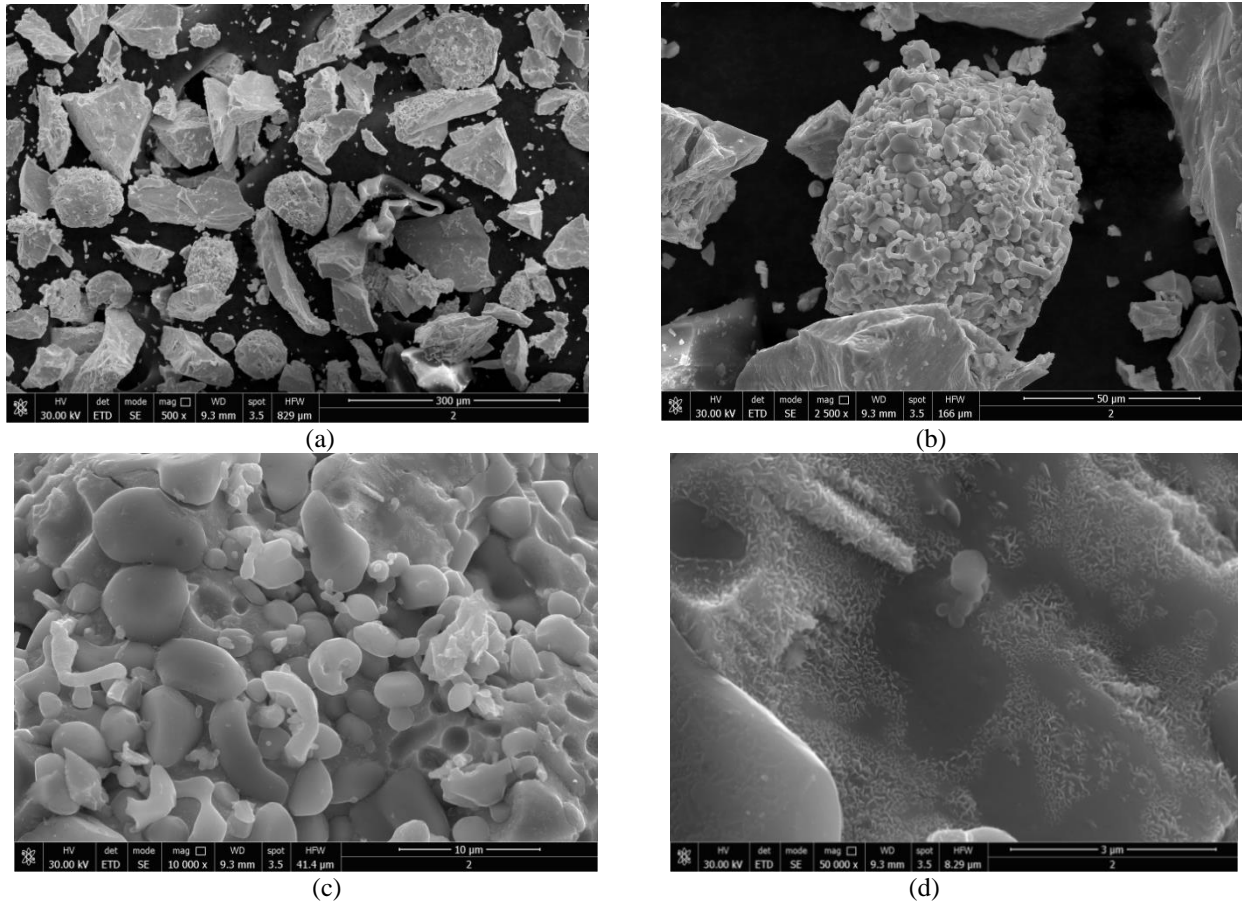


Fig. 2(a-d) present the SEM images of β - Zn_4Sb_3 which reveal dense areas of the materials and also a certain grade of porosity.

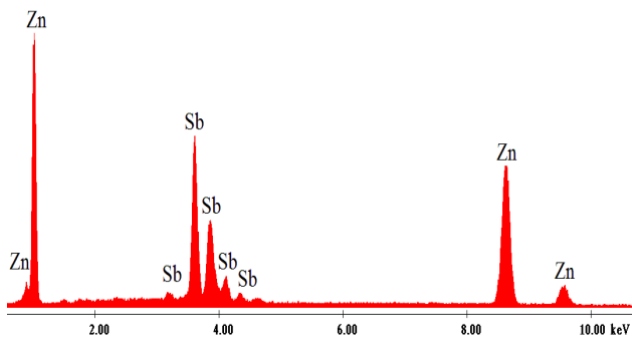


Fig. 3. EDX image of Zn_4Sb_3

This porosity may affect by presence, the mechanical strength of the material. Pedersen [31] has showed that the material density influences the thermoelectric properties more than doping, the figure of merit increasing with density.

From the EDX spectrum (Fig. 3) is noticed only the presence of the zinc and antimony ions.

Also, the EDX spectrum shows the characteristic lines [32] of the Zn and Sb as it follows: for Zn - $K_{\alpha 1}$ at 8.63 KeV, $K_{\beta 1}$ at 9,6KeV, $L_{\alpha 1}$ at 1,01KeV and for Sb - $L_{\alpha 1}$ at 3.60, $L_{\beta 1}$ at 3.84KeV and $L_{\beta 2}$ at 4.1KeV.

Using the atomic force microscopy, the surfaces topography was analyzed, the measures being realized in the contact mode on a scanned surface of $9\mu m \times 9\mu m$ processing the experimental data with the NanoSurf EasyScan2 soft.

It was observed that the agglomerations produced on the scanned surface are about 79 (Fig. 4.).

The measured particles dimension on the scanned surfaces is between 2.1 and 3.2 μm .

In Fig.5. is presented the AFM image of the analyzed Zn_4Sb_3 sample representing the surface topography and in Fig. 6 is represented the color map of the sample. In Fig.7. is presented the AFM image of the 3D topographical map of the Zn_4Sb_3 material.

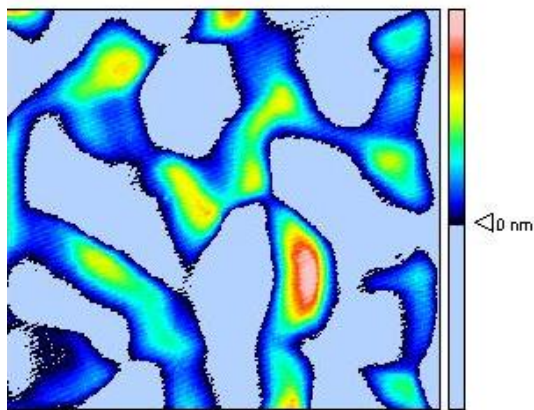


Fig. 4. The islands characteristics

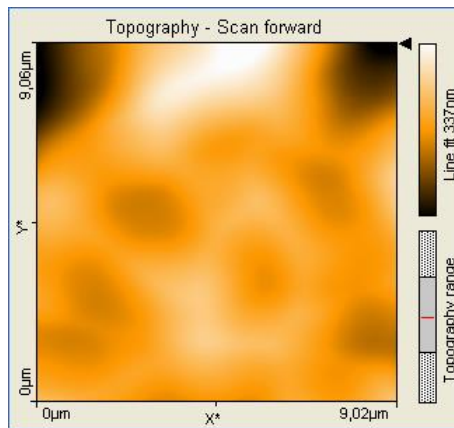


Fig. 5. The AFM image of Zn_4Sb_3 representing the surface topography.

Also, the average surface roughness - S_a and the root mean squared surface roughness - S_q were determined for an area $A=82.36\mu m^2$.

The equations used for the average surface roughness and the root mean squared surface roughness's calculations are [33]:

$$S_a = \frac{1}{mn} \sum_{j=1}^n \sum_{i=1}^m |z_{ij}| \quad (2)$$

$$S_q = \sqrt{\frac{1}{mn} \sum_{i=1}^m \sum_{j=1}^n z^2(x_i, y_j)} \quad (3)$$

where m and n represent the number of the particles on x and y axis, with z -the medium high of the particles, x_k and y_l represent the minimum and the maximum deviations of the particles related to the medium value.

For Zn_4Sb_3 , were measured: $S_a = 39nm$ and $S_q = 55nm$.

To form a better opinion about the topography of the obtained material Zn_4Sb_3 , a 3D representation in 2D map of Zn_4Sb_3 was built using the NanoSurf EasyScan2 soft, as it can be seen in Fig.8.

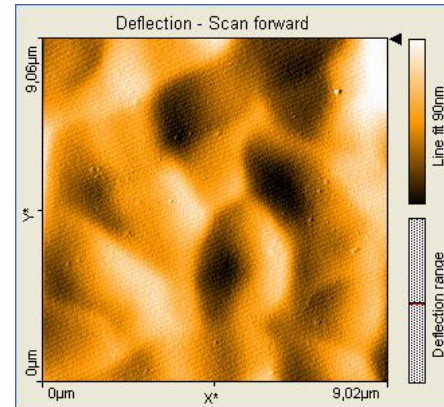


Fig. 6. The AFM image of Zn_4Sb_3 representing the color map of the scanned surface.

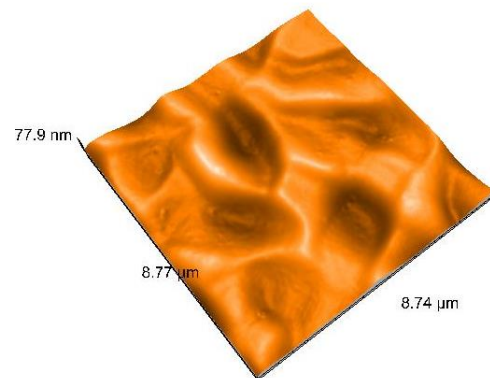


Fig.7. The AFM image of Zn_4Sb_3 representing the 3D topographical map of the Zn_4Sb_3 material.

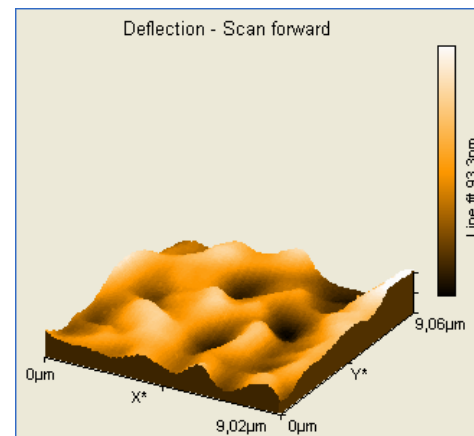


Fig.8. The AFM image of Zn_4Sb_3 representing the 3D representation in 2D map of the Zn_4Sb_3 material.

4. Conclusions

In this paper were presented the successfully results of the obtaining Zn_4Sb_3 by melting Zn and Sb precursors of high purity. The compound was obtained by mixing Zn and Sb in a stoichiometric 4:3 ratio, followed by melting the mixture at 1173 K for 24 hours in an sealed ampoule with a vacuum environment.

The X-Ray diffraction patterns shows that the β -Zn₄Sb₃ phase was formed.

A morphology study of the compound was made using the Scanning Electron Microscopy and the Atomic Force Microscopy techniques. The studies revealed that the particles are agglomerated and assymmetric forming dense areas of the materials combined with a certain degree of porosity. The energy-dispersive X-ray spectroscopy analysis shows that the compound contain only Zn and Sb atoms, the characteristic peaks of Zn and Sb being identified.

Using the Atomic Force Microscopy, the particles dimension on the scanned surfaces was determined to be between 2.1 and 3.2 μm . The average surface roughness - S_a and the root mean squared surface roughness - S_q were determined for an area $A=82.36\text{pm}^2$: $S_a = 39\text{nm}$ and $S_q = 55\text{nm}$.

Acknowledgement

„This work was partially supported by the strategic grant POSDRU/159/1.5/S/137070 (2014) of the Ministry of National Education, Romania, co-financed by the European Social Fund – Investing in People, within the Sectoral Operational Programme Human Resources Development 2007-2013.”

The authors thank to the X-ray Diffraction and Atomic Force Microscopy Laboratories from the Characterization Department of the National Institute for Research and Development in Electrochemistry and Condensed Matter (Timisoara, Romania) and to the Electron Microscopy Laboratory from the Research Institute for Renewable Energy (Timisoara, Romania) for the characterization results.

References

- [1] T. Caillat, J.P. Fleurial, A. Borschevsky, *J. Phys. Chem. Solids* **58** (7), 1119 (1997).
- [2] B. L. Pedersen, B. B. Iversen, *Appl. Phys. Lett.* **92**, 161907 (2008).
- [3] V. Izard, M.C. Record, J.C. Tedenac, S.G. Fries, *Calphad* **25**, 567 (2002).
- [4] H.W. Mayer, I. Mikhail, K. Schubert, *J. Less Common Met.* **59**, 43 (1978).
- [5] G.J. Snyder, E.S. Toberer, *Nat. Mater.* **7**, 105 (2008).
- [6] D. Tang, W. Zhao, S. Cheng, P. Wei, J. Yu, Q. Zhang, *J. Solid State Chem.* **193**, 89 (2012).
- [7] P. H. M. Bottger, S. Diplas, E. Flage-Larsen, Ø. Prytz, T. G. Finstad, *J. Phys. Condens. Matter.* **23**, 265502 (2011).
- [8] D. Li, X.Y. Qin, *Intermetallics* **19**(11), 1651 (2011).
- [9] P. Rauwel, O.M. Løvvik, E. Rauwel, J. Taftø, *Acta Mater.* **59**, 5266 (2011).
- [10] X. Shai, S. Deng, D. Meng, L. Shen, D. Li, *Phys. B* **452**, 148 (2014).
- [11] S. Bhattacharya, R. P. Hermann, V. Keppens, T. M. Tritt, G. J. Snyder, *Phys. Rev. B* **74**, 134108 (2006).
- [12] E. S. Toberer, P. Rauwel, S. Gariel, J. Taftø, G. J. Snyder, *J. Mater. Chem.* **20**, 9877 (2010).
- [13] D. Cadavid, J. E. Rodriguez, *Physica B* **403**, 3976 (2008).
- [14] K. Ueno, A. Yamamoto, T. Noguchi, T. Inoue, S. Sodeoka, H. Obara, *J. Alloys Compd.* **392**, 295 (2005).
- [15] Z.H. Zheng, P. Fan, P.J. Liu, J.T. Luo, G.X. Liang, D.P. Zhang, *J. Alloys Compd.* **594** (5), 122 (2014).
- [16] C. Stiewe, T. Dasgupta, L. Bottcher, B. Pedersen, E. Muller, B. Iversen, *J. Electronic Mater.* **39**(9) 1975 (2010).
- [17] D. Qi, X. Tang, H. Li, Y. Yan, Q. Zhang, *J. Electronic Mater.* **39** (8), 1159 (2010).
- [18] B. Gault, E. A. Marquis, D. W. Saxe, G. M. Hughes, D. Manginck, E. S. Toberer, G. J. Snyder, *Scripta Mater.* **63**, 784 (2010).
- [19] B. Poudel, Q. Hao, Y. Ma, Y. Lan, A. Minnich, B. Yu, X. Yan, D. Wang, A. Muto, D. Vashaev, X. Chen, J. Liu, M.S. Dresselhaus, G. Chen, *Z. Ren, Science* **320**, 634 (2008).
- [20] G. Nakamoto, K. Kinoshita, M. Kurisu, *J. Alloys Compd.* **436**, 65 (2007).
- [21] Ø. Prytz, A.E. Gunnæs, O.B. Karlsen, T.H. Breivik, E.S. Toberer, G. Jeffrey Snyder, J. Taftø, *Phil. Mag. Lett.* **89**(6), 362 (2009).
- [22] C. Okamura, T. Ueda, K. Hasezaki, *Mater. Trans.* **51**(1), 152 (2010).
- [23] D. T. K. Anh, T. Tanaka, G. Nakamoto, M. Kurisu, *J. Alloys Compd.* **421**, 232 (2006).
- [24] A. Denoix, A. Solaiappan, R.M. Ayril, F. Rouessac, J.C.Tedenac, *J. Solid State Chem.* **183**, 1090 (2010).
- [25] H. Yin, M. Christensen, B.L. Pedersen, E. Nishibori, S. Aoyagi, B.B. Iversen, *J. Electronic Mater.* **39**(9), 1957 (2010).
- [26] T. Dasgupta, C. Stiewe, A. Sesselmann, H. Yin, B. B. Iversen, E. Mueller, *J. Appl. Phys.* **113**, 103708 (2013).
- [27] Y. Mozharivskiy, A. O. Pecharsky, S. Bud'ko, G. J. Miller, *Chem. Mater.* **16**, 1580 (2004).
- [28] G. Zhu, W. Liu, Y. Lan, G. Joshi, H. Wang, G. Chen, *Z. Ren, Nano Energy* **2**, 1172 (2013).
- [29] M. Tapiero, S. Tarabichi, J. G. Gies, C. Noguét, J. P. Zielinger, M. Joucla, J. Loison, M. Robino, J. Henrion, *Solar Energy Mater.* **12**, 257 (1985).
- [30] F. Rouessac, R.M. Ayril, *J. Alloys Compd.* **530**, 56 (2012).
- [31] B. L. Pedersen, H. Birkedal, B. B. Iversen, M. Nygren, P. T. Frederiksen, *Appl. Phys. Lett.* **89**, 242108 (2006).
- [32] S. Sitthichai, T. Thongtem, S. Thongtem, T. Suriwong, *Superlattices Microstruct.* **64**, 433 (2013).
- [33] D. Johnson, N. Hilal, *Desalination* **356**, 149 (2015).

*Corresponding author: voida.mirela@yahoo.com